

A 50-EW/cm² Ti:sapphire laser system for studying relativistic light-matter interactions

Barry C. Walker^{a)}, Csaba Tóth^{b)}, David N. Fittinghoff^{b)}, Ting Guo^{c)},
Dong-Eon Kim^{d)}, Christoph Rose-Petruck^{e)}, Jeff A. Squier^{f)},
Koichi Yamakawa^{g)}, Kent R. Wilson, and C.P.J. Barty^{h)}

Department of Chemistry and Biochemistry, University of California San Diego, La Jolla, CA 92093, USA

- a) Present address: Department of Physics and Astronomy, University of Delaware, Newark, DE 19716, USA
b) UCSD affiliation: The Institute for Nonlinear Science
c) Present address: Department of Chemistry, University of California Davis, Davis, CA 95616, USA
d) Present address: Pohang University of Science and Technology, Pohang, 790-784, Republic of Korea
e) Present address: Department of Chemistry, Brown University, Providence, RI 02912, USA
f) UCSD affiliation: Department of Electrical and Computer Engineering
g) Present address: Advanced Photon Research Center, KANSAI-JAERI, Kyoto 619-0215, Japan
h) UCSD affiliation: Department of Applied Mechanics/Engineering Sciences

e-mail contact: cxt@chem.ucsd.edu, jas@chem.ucsd.edu, bcwalker@udel.edu, cpjb@chem.ucsd.edu

Abstract: A 10-Hz repetition rate, 60-TW peak power, Ti:sapphire laser system was developed for use in experiments where relativistic effects dominate the physics. The temporal, spectral, energy and spatial characteristics of the laser pulses were measured in single shot format. The pulse duration ranged from 22 fs to 25 fs and the pulse energy averaged 1.3 J. Atomic photoionization measurements quantified the peak intensity of the laser pulse *in situ*. The measurements indicated an intensity of at least 5×10^{19} W/cm² was produced.

©1999 Optical Society of America

OCIS codes: (320.7090) Ultrafast lasers; (140.3590) Lasers, titanium; (140.3280) Laser amplifiers

References and links

1. M. D. Perry, G. Mourou, "Terawatt to petawatt subpicosecond lasers," *Science* **264**, 917-923 (1994).
2. H.R. Reiss, "Relativistic Effects in Strong Electromagnetic Fields," *Opt. Exp.* **2**, 261-297 (1998), <http://www.opticsexpress.org/opticsexpress/framestocv2n7.htm>
3. A. Sullivan, H. Hamster, H. C. Kapteyn, S. Gordon, W. White, H. Nathel, R. J. Blair, R. W. Falcone, "Multiterawatt, 100-fs laser," *Opt. Lett.* **16**, 1406-1408 (1991).
4. C.P.J. Barty, C.L. Gordon III, B.E. Lemoff, "Multiterawatt 30-fs Ti:sapphire laser system," *Opt. Lett.* **19**, 1442-1444 (1994).
5. J. P. Chambaret, C. L. Blanc, G. Chériaux, P. Curley, G. Darpentigny, P. Rousseau, G. Hamoniaux, A. Antonetti, F. Salin, "Generation of 25-TW, 32-fs pulses at 10 Hz," *Opt. Lett.* **21**, 1921-1923 (1996).
6. A. Antonetti, F. Blasco, J. P. Chamberet, G. Chériaux, G. Darpentigny, C. Le Blanc, P. Rousseau, S. Ranc, G. Ray, F. Salin, "A laser system producing 5×10^{19} W/cm² at 10 Hz," *Applied Physics B* **65**, 197 (1997).
7. S. Backus, C. G. Durfee, III, M. M. Murnane, H. C. Kapteyn, "High power ultrafast lasers," *Rev. Sci. Inst.* **69**, 1207-1223 (1998).
8. K. Yamakawa, M. Aoyama, S. Matsuoka, H. Takuma, D. Fittinghoff, C.P.J. Barty, "Generation of 16-fs, 10-TW pulses at 10 Hz repetition rate with efficient Ti:sapphire amplifiers," *Opt. Lett.* **23**, 1468-1470 (1998).
9. K. Yamakawa, M. Aoyama, S. Matsuoka, T. Kase, Y. Akahane, H. Takuma, "100-TW, sub-20-fs Ti:sapphire laser system operating at a 10-Hz repetition rate," *Opt. Lett.* **23**, 1468-1470 (1998).
10. G. A. Mourou, C.P.J. Barty, M. D. Perry, "Ultrahigh-intensity lasers: physics of the extreme on the tabletop," *Physics Today*, **51** (1), 22-28 (1998).
11. J. D. Kmetec, C. L. Gordon III, J. J. Macklin, B. E. Lemoff, G. S. Brown, and S. E. Harris, "MeV x-ray generation with a femtosecond laser," *Phys. Rev. Lett.* **68**, 1527-1530 (1992).
12. S.Y. Chen, A. Maksimchuk, D. Umstadter, "Experimental observation of relativistic nonlinear Thomson scattering," *Nature* **396**, 653-655 (1998).
13. C. Rose-Petruck, R. Jimenez, T. Guo, A. Cavalleri, C. W. Siders, F. Raksi, J. A. Squier, B. C. Walker, K. R. Wilson, C. P. J. Barty, "Picosecond-milliangstrom lattice dynamics measured by ultrafast X-ray diffraction," *Nature* **398**, 310-312 (1999).

14. C. Rischel, A. Rousse, I. Uschmann, P. A. Albouy, J. P. Geindre, P. Audebert, J. C. Gauthier, E. Förster, J. L. Martin, A. Antonetti, "Femtosecond time-resolved X-ray diffraction from laser-heated organic films," *Nature* **390**, 490-492 (1997).
15. D. Kim, C. Tóth, C. P. J. Barty, "Population inversion between atomic inner-shell vacancy states created by electron-impact ionization and Coster-Kronig decay," *Phys. Rev. A* **59**, R4129-4132 (1999).
16. C.I. Moore, J.P. Knauer, D.D. Meyerhofer, "Observation of the transition from Thomson to Compton-scattering in multiphoton interactions with low-energy electrons," *Phys. Rev. Lett.* **74**, 2439-2442 (1995).
17. Y. Ueshima, Y. Kishimoto, A. Sasaki, T. Tajima T, "Laser Larmor X-ray radiation from low-Z matter," *Laser and Particle Beams* **17**, 45-58 (1999).
18. J. Zhou, G. Taft, C.P. Huang, M.M. Murnane, H.C. Kapteyn, "Pulse evolution in a broad-bandwidth Ti:sapphire laser," *Opt. Lett.* **19**, 1149-1167 (1994).
19. C. Spielmann, P. F. Curley, T. Brabec, and F. Krausz, "Ultrabroadband femtosecond lasers," *IEEE J. Quant. Elec.* **30**, 1100-1114 (1994).
20. D. Strickland, G. Mourou, "Compression of amplified chirped optical pulses," *Opt. Comm.* **56**, 219-221 (1985).
21. B. E. Lemoff, C. P. J. Barty, "Quintic-phase-limited, spatially uniform expansion and recompression of ultrashort optical pulses," *Opt. Lett.* **18**, 1651-1653 (1993).
22. See, e.g. D. N. Fittinghoff, B. C. Walker, J. A. Squier, C. S. Tóth, C. Rose-Petruck, C. P. J. Barty, "Dispersion considerations in ultrafast CPA systems," *IEEE J. Sel. Top. Quant. Elec.* **4**, 430-40 (1998).
23. C. P. J. Barty, T. Guo, C. L. Blanc, F. Ráksi, C. Rose-Petruck, J. Squier, K. R. Wilson, V. V. Yakovlev, K. Yamakawa, "Generation of 18-fs, multiterawatt pulses by regenerative pulse shaping and chirped-pulse amplification," *Opt. Lett.* **21**, 668-670 (1996).
24. B. C. Walker, J. A. Squier, D. N. Fittinghoff, C. Rose-Petruck, C. P. J. Barty, "Hybrid vacuum-atmosphere compressors for ultrafast, high-peak power chirped-pulse amplification," *IEEE J. Sel. Top. Quant. Elec.* **4**, 441-444 (1998).
25. D. J. Kane, R. Trebino, "Single-shot measurement of the intensity and phase of an arbitrary ultrashort pulse by using frequency-resolved optical gating," *Opt. Lett.* **18**, 823-825 (1993).
26. C. Tóth, D. N. Fittinghoff, B. C. Walker, J. A. Squier, C. P. J. Barty, "Pulse characterization techniques for sub-30 femtosecond terawatt lasers," *Ultrafast Phenomena XI* (Springer-Verlag) **63**, 109-111 (1999).
27. B. C. Walker, C. Tóth, D. N. Fittinghoff, T. Guo, "Theoretical and experimental spectral phase error analysis for pulsed laser fields," *J. Opt. Soc. Am. B* **16**, 1292-1299 (1999).
28. B. Walker, B. Sheehy, L. F. DiMauro, P. Agostini, K. J. Schafer, K. C. Kulander, "Precision measurement of strong field double ionization of helium," *Phys. Rev. Lett.* **73**, 1227-1230 (1994).
29. S. Augst, D.D. Meyerhofer, D. Strickland, S.L. Chin, "Laser ionization of noble gases by Coulomb-barrier suppression," *J. Opt. Soc. Am. B* **8**, 858-867 (1991).
30. M.V. Ammosov, N.B. Delone, V.P. Krainov, "Tunnel ionization of complex atoms and of atomic ions in an alternating electromagnetic field," *Sov. Phys. JETP* **64**, 1191-1194 (1986).

1. Introduction

Intense ultrashort laser pulses have been heralded as the light source for future fundamental light-matter studies at ultrahigh intensities. Experiments using these laser pulses are expected to continue to extend light-matter interactions into relativistic, strong field phenomena [1,2]. Several laboratories have constructed new laser systems that produce sub-100-fs duration pulses with up to 100 TW of peak power [3-9]. Interesting scientific results achieved with these lasers in the fields of high order harmonic and short pulse X-ray generation, high density plasmas, relativistic acceleration, relativistic nonlinear optics, time resolved X-ray diffraction and absorption, etc., are emerging [10-14]. In this paper, we present a Ti:sapphire laser amplifier system specifically designed for fundamental high-field interaction studies and laser based X-ray generation [15-17]. 20 femtosecond pulse amplification to the multiterawatt level pushes the limits of the current technology in many aspects. Technical issues, which must be considered in detail with ultrafast terawatt amplifiers, are described here. Because a physical understanding of non-perturbative light-matter interactions depends on the laser intensity, we performed high-field atomic photoionization experiments to accurately measure, *in situ*, the peak intensity of the laser pulse.

2. A 50 THz bandwidth, 60 TW peak-power, Ti:sapphire laser system

The laser system can be described in three sections: generation and shaping of the initial pulse, amplification, and compression and measurement of the amplified pulse. In the interest of providing an accurate presentation of the system and detailed information needed for a full analysis, high-resolution photographic images are included in Figure 1.

2.1. Oscillator, pulse stretcher, and initial system considerations

A mode-locked oscillator produces the nascent low energy pulse in the laser system. The most important characteristic of the initial ultrafast pulse is its ability to serve as a large-bandwidth, "Fourier-transform limited" source. The Ti:sapphire oscillator used in our laser system (Fig. 1a) employs fused silica prism dispersion compensation [18,19]. The oscillator was pumped by an intra-cavity doubled, diode-pumped Nd:vanadate laser (Millennia V, Spectra Physics) at 1.4 W and produced ~ 15 -fs pulses with 2 nJ of energy and a FWHM bandwidth exceeding 115 nm centered at 800 nm. The duration of the oscillator pulses was measured using a balanced fringe-resolved autocorrelator.

Amplification of the initial oscillator pulse at maximum efficiency stipulates the amplifiers be operated above the $1\text{-J}/\text{cm}^2$ saturation fluence of the Ti:sapphire gain medium. By contrast, the damage threshold of the amplifier components requires they be operated below approximately $5\text{ GW}/\text{cm}^2$. The chirped pulse amplification technique [20] has been extremely successful at resolving this problem by stretching the pulse before amplification. In our system, very large stretching ratios are achieved by passing the oscillator pulse through the stretcher four times with a beam inversion between the second and third pass (see green outlined inversion optics platform in Fig. 1b). Our stretcher was modified from an earlier construction [21] by using a 50.2 degree angle of incidence on 1200 line/mm ruled gratings (Milton Roy, master MR 136). Temporal shaping (i.e. spectral "chirping") of the 15-fs pulse reduces the $0.5\text{-MW}/\text{cm}^2$ initial peak intensity to $10\text{ W}/\text{cm}^2$ by stretching the pulse in time to ~ 0.8 ns, and increasing the safe amplification range by almost five orders of magnitude.

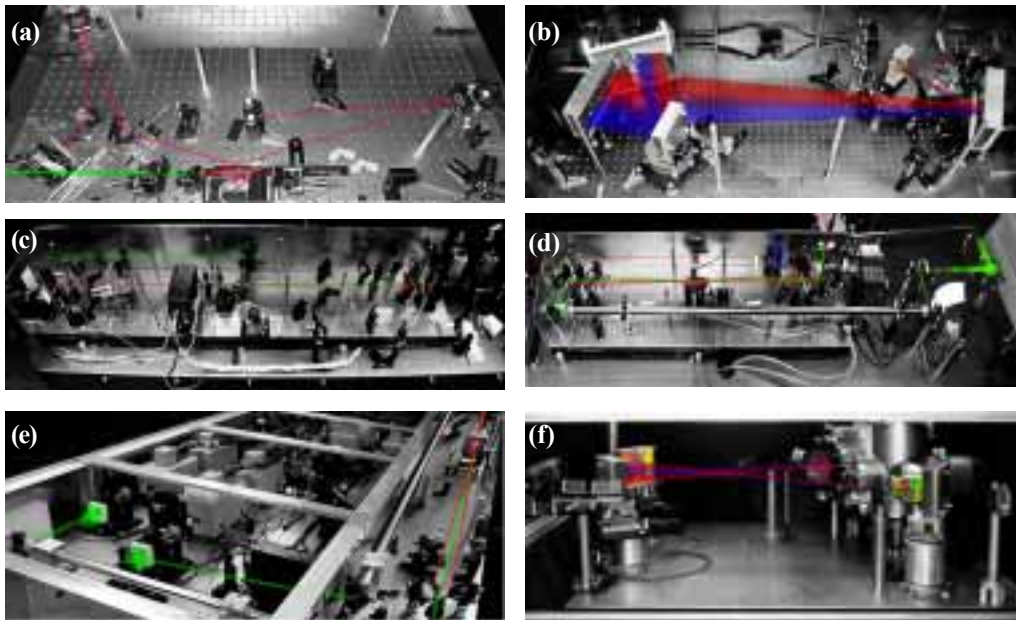


Figure 1: Picture schematics of (a) oscillator, (b) off-axis stretcher, (c) regenerative amplifier, (d) 4-pass amplifier, (e) final-amplifier, and (f) hybrid vacuum compressor. Zoom to take advantage of high resolution. Scale indicated by 1" bolt pattern on optical tables.

Implementing CPA for a ten-optical-cycle pulse and joule level energy presents special challenges due to the 50 THz pulse bandwidth and sheer magnitude of the laser system. To maintain temporal fidelity during the amplification of this bandwidth, the laser system was carefully modeled. In our laser system design, spectral phase distortions [22] were computationally minimized by iterative optimization of the angle of incidence in the off-axis cylindrical mirror stretcher, the amplifier component composition, and the compressor grating angle and separation. During the laser construction, experimental adjustments of the amplifier material paths and compressor were made to correct for variations from the calculated spectral

phase. Successful optimization ultimately entailed controlling the spectral phase to within 1 radian across the pulse bandwidth. The dispersive elements in the optical path include: e-sapphire (25 cm); o-quartz (4 mm), o-KD*P (36 cm); terbium-gallium-garnet (21 mm); BK7 (0.5 m); protected Ag metal mirrors (20 bounces); normal incidence $\lambda/4$ HfO₂/SiO₂ mirrors (24 bounces); 45 degree, s-wave $\lambda/4$ HfO₂/SiO₂ mirrors (25 bounces); angle-tuned, thin, 12% s-polarization reflectivity etalon (24 passes) used at antiresonance and single pass effective thickness of $13\times\lambda/4$; and 70 m of air.

To prevent the potentially catastrophic amplification of a "bad" pulse, from the oscillator, or an optical misalignment, three quality control mechanisms were employed. First, the system was housed within HEPA-filtered, dust-reducing environment and contiguously double boxed to decrease air currents. Second, the repetition rate of the mode locked oscillator was continuously monitored. In the event of instability in the mode-locked pulse train, the laser system was shut down prior to the amplification of the pulse. Third, the optical alignment between the subsequent stages and the pulse spectrum were continuously monitored at each amplification stage with CCD cameras.

2.2. Amplifier stages

Amplification of the pulse energy from 80 pJ to 2.6 J is accomplished in three stages. The $>10^{12}$ gain in amplification requires special attention to spectral amplitude issues (e.g. gain narrowing) in addition to the aforementioned spectral phase. Furthermore, a high quality spatial mode for the pulse was needed to yield the greatest focused intensity. The amplifier designs were optimized using a model that included thermal lensing, spatial and temporal gain profiles, and propagation. The amplifier configuration was optimized taking into consideration optical damage thresholds, mode quality, component minimization, and conversion efficiency. Small adjustments to the amplifier components (e.g. lens values and positions) were made during the construction of the system to experimentally maximize performance. For the reasons cited above, i.e., to amplify a high quality spatial mode while simultaneously minimizing spectral narrowing, the first 4×10^7 amplification is done in a stable TEM₀₀ cavity regenerative amplifier (Fig. 1c). One cavity end mirror was flat and the other had a concave 10 m radius. An intracavity Pockels cell (Cleveland Crystals, Medox DR-85A driver) and thin film polarizer (Alpine Research Optics) were used to inject a pulse into the amplifier cavity. After 12 roundtrips in the cavity the Pockels cell was again energized to switch the pulse out of the cavity. During switching, the Pockels cell is in a half-wave retardation for approximately 5 ns, otherwise, the Pockels cell retardation is zero. The regenerative amplifier is pumped by a frequency doubled, Q-switched, flashlamp pumped, Nd:YAG laser (Continuum, model 6020). An intra-cavity nitrocellulose pellicle etalon (thickness 1.6 μm , angle of incidence $\sim 50^\circ$) is used at near antiresonance to compensate for spectral gain narrowing and gain saturation effects during amplification [23]. The amplified FWHM pulse spectrum is given in Table 1.

Table 1. Representative pulse parameters along the Ti:sapphire amplifier chain

	Oscillator	Stretcher	Regen	4-pass	2-pass	Compressor
Repetition rate (Hz)	8×10^7	8×10^7	20	20	10	10
Pump energy (J)	1.4/s	N/A	0.075	0.75	5.2	N/A
Pulse energy (J)	2×10^{-9}	8×10^{-11}	3×10^{-3}	0.28	2.6	1.3
Beam diameter (mm)	0.9	1.7	1	4.2	10	50
Spectrum FWHM (nm)	115	115	100	85	75	75

A 4-pass "bow-tie" amplifier follows the regenerative amplifier. The output beam of the regenerative amplifier was matched to a 4-pass amplifier (Fig. 1d) gain volume with a 10 m focal length lens (blue outline Fig. 1d). This amplifier was pumped by a frequency doubled Q-switched Nd:YAG laser (Continuum, model 9020). The 532 nm pump beam was split into two vertically flipped beams that were demagnified to a 5.5 mm diameter and vacuum relay imaged to each face of a 12 mm diameter, 18 mm length, normal incidence, MgF₂ antireflection coated, Ti:sapphire amplifier rod (see Fig 1d). The conversion of the absorbed

pump energy to 800 nm pulse energy was 37% for this amplifier. The emphasis was placed on beam quality. The pump energy absorbed in the gain medium is given with the pulse energy at each stage of amplification in Table 1.

The output from the 4-pass amplifier was expanded and matched to the gain medium of a final 2-pass amplifier (Fig. 1e) with a two lens telescope (-1.5 m and 10 m focal length). The 2-pass amplifier is pumped by two beams from a frequency doubled Q-switched Nd:YAG laser (Continuum). The pump light had a super gaussian intensity distribution 11 mm in diameter, with 10% peak-to-peak amplitude variation. The pump light was vacuum relay imaged (unity magnification) from the doubling crystals of the pump laser to each face of a 30 mm diameter, 30 mm length Ti:sapphire gain medium (Crystal Systems). The 2-pass amplifier converts 50% of the absorbed pump energy into the final pulse energy. The near-field intensity distribution is shown in Fig. 2a and Fig. 2b. The final, shot-to-shot pulse energy distribution (Fig. 2c) has a mean energy value of 2.6 J with $\pm 7\%$ fluctuations. 50% conversion corresponds to 90% of the theoretical maximum energy extraction.

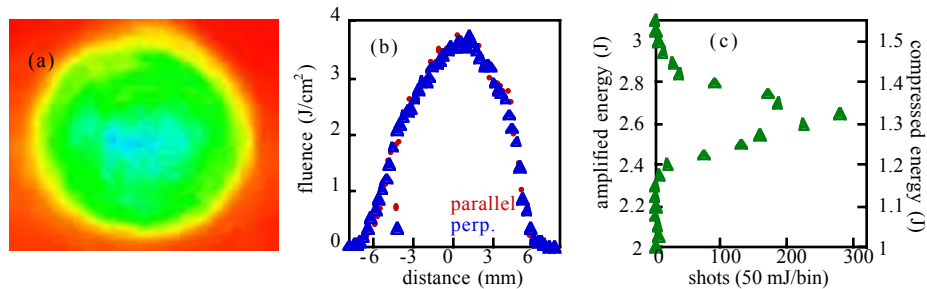


Figure 2: Amplified beam in 2-D (a), line-out (b), and integrated pulse energy histogram (c).

2.3. Pulse compression and peak intensity

The output from the 2-pass amplifier is expanded, by a factor of five, with an off-axis reflective Galilean telescope. The highest intensity and average power density of the pulses in the compressor was 2.5 TW/cm^2 and 1.5 W/cm^2 , respectively. Because the final pulse exceeds the intensity where nonlinear light-matter interactions occur in the atmosphere, the pulse compression and delivery to the target area must be in vacuum. A hybrid atmosphere-vacuum compressor [24] was used to allow compact compression of the laser pulse in an oil-free vacuum environment (Fig. 1f). The group delay of the hybrid system was the same as an 'all-vacuum' compressor within 1 fs precision. The spectral amplitude and phase properties of the amplified pulses were measured using a 5×10^5 contrast, low-dispersion, single-shot PG-FROG frequency resolved optical gating (FROG) [25,26]. We used FROG to optimize the laser system dispersion. Atmospheric control of the grating stages allowed experimental optimization of the hybrid vacuum compressor. As an example of the optimization, and to convey the sensitivity of the pulse, single-shot FROGs as a function of the grating separation are shown in Fig. 3a. The movie begins with several shots acquired at the optimal compressor setting (63 degree angle of incidence on the grating, 115 cm grating separation), to convey the pulse to pulse fluctuations of the system. After these shots, the movie contains FROGs corresponding to grating positions a distance Δd from the optimum. The final energy of the pulse after compression averaged 1.3 J/shot with a $\pm 7\%$ standard deviation (Fig. 2c). Several million full power laser shots were fired without detectable damage to the final grating. In part, this is the result of the cleanliness of the smaller vacuum environment. The retrieved pulses had a mean FWHM pulse duration of 23.5 fs, with measured values ranging from 22-25 fs. The accuracy of the retrieved pulses can be seen from the agreement between the experimental and retrieved time marginals in Fig. 3b. The time marginal, shown in Fig. 3b over a dynamic range of 10^5 , is the third-order autocorrelation of the pulse. The retrieved spectral intensity and phase are shown in Fig. 3c and Fig. 3d, respectively. The intensity weighted RMS spectral phase error [27] for the optimal pulse (Fig. 3b-d) is only 0.4 radian, corresponding to roughly 1.4 times the transform limit.

The peak intensity that our laser can produce is one of its most important assets. In order to estimate the peak intensity achievable when the laser is focused, we have measured the spatial profile of the attenuated pulse when focused by a 45 degree, 0.2-wave distortion, off axis silver or gold coated parabola (II-IV, Inc). The parabola section was 11.4 cm in diameter and had a focal length of 10 cm. At best focus, the FWHM of the beam along and perpendicular to the laser polarization is 1.4 and 1.3 times, respectively, that of a TEM₀₀ beam of the same input FWHM diameter. The FWHM diameter at the focal spot is 3 ± 0.4 μm . To obtain the optimal focus, 0.05 mrad experimental adjustments of the tilt, rotation, and groove alignment for the compressor gratings were required. Despite this level of adjustment accuracy, an estimated 40% of the spatial aberrations in the final beam were chromatic. Combining the results of pulse energy, pulse duration and focal spot measurements, one predicts that peak laser intensity in excess of 10^{20} W/cm² is possible with the laser system described. However, this estimation can be quite inaccurate due to error accumulation from independent optical measurements, unaccounted spatial chirp, or energy in the spatial and temporal wings of the pulse. A more direct measurement was needed to determine the actual peak laser intensity.

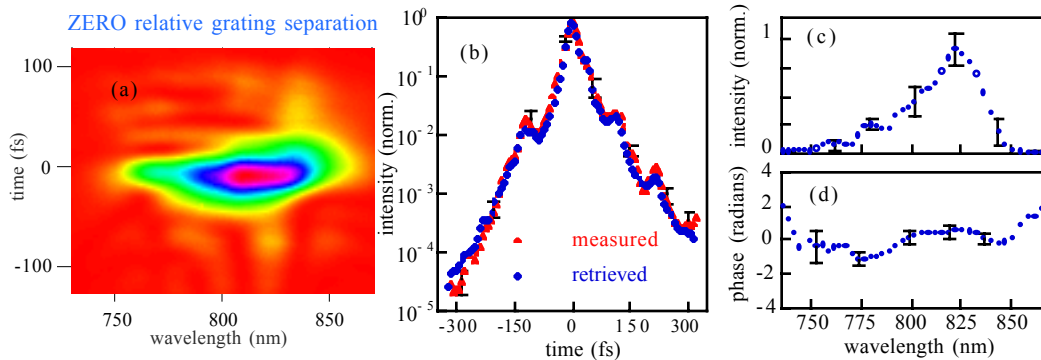


Figure 3: (a) FROG traces as a function of compressor separation (0.29 Mb QuickTime animation). The mean time marginal (b), retrieved pulse spectrum (c) and spectral phase (d) are also shown. The error bars shown are one standard deviation of the single shot values.

Photoionization experiments were done to more accurately measure the ion charge distribution from the laser focus in a low-density (10^{-8} Torr) noble gas (He, Ne, Ar) [28,29]. The experimental apparatus and results will be presented in detail in a future publication. Briefly, the light entered the chamber via a 10 μm thick pellicle window, and was focused by a parabola identical to the one used in the beam profile measurements. An 0.1 mm diameter effusive gas jet delivered the atoms to the focal region. Atoms photoionized by the light were extracted from the interaction region with field plates and analyzed with a time-of-flight spectrometer. Typical sample pressures in the interaction region are 10^{-8} Torr. The background pressure was 10^{-11} Torr. For helium, attenuated beam energies of 50 μJ saturated the strong field photoionization process. Intensity calibrations from studies for helium [28], known to be accurate to 15%, were adjusted for the decreased pulse duration in this experiment, and place the intensity calibration at 1.4×10^{15} W/cm² for 50 μJ of energy. To test the focused intensity at full power, argon was used as a sample gas. In these experiments, saturation of Ar¹⁶⁺ was observed near the full pulse energy. Using the tunneling ionization rates for this species [30] an intensity of $>5\times 10^{19}$ W/cm² would have to be reached in our experiment to ionize argon to the 1s² electronic state observed. This is a lower bound on the intensity. The upper bound is the intensity necessary to reach the hydrogen-like ionization species which is $>10^{21}$ W/cm².

3. Summary

We have developed an ultrafast Ti:sapphire laser system that can produce 60 TW peak power pulses at a high repetition rate, with low pulse-to-pulse fluctuations. The focused intensity of the laser was measured to be 5×10^{19} W/cm². The laser is suitable for studies in the intensity regime above 10^{18} W/cm² where relativistic physics dominates the light-matter interaction.